



© 2020 Geological Society of America. For permission to copy, contact editing@geosociety.org

https://doi.org/10.1130/G47253.1

Manuscript received 25 November 2019 Revised manuscript received 27 February 2020 Manuscript accepted 13 March 2020

Published online 29 April 2020

# Pliocene–Pleistocene megafloods as a mechanism for Greenlandic megacanyon formation

Benjamin A. Keisling<sup>1</sup>, Lisbeth T. Nielsen<sup>2</sup>, Christine S. Hvidberg<sup>2</sup>, Roman Nuterman<sup>2</sup> and Robert M. DeConto<sup>1</sup> Climate System Research Center, Department of Geosciences, University of Massachusetts–Amherst, Amherst, Massachusetts 01003, USA

<sup>2</sup>Centre for Ice and Climate, Physics of Ice, Climate and Earth, Niels Bohr Institute, University of Copenhagen, 2100 Copenhagen, Denmark

#### ABSTRACT

The Greenland ice sheet (GrIS) covers a complex network of canyons thought to be preglacial and fluvial in origin, implying that these features have influenced the ice sheet since its inception. The largest of these canyons terminates in northwest Greenland at the outlet of the Petermann Glacier. Yet, the genesis of this canyon, and similar features in northern Greenland, remains unknown. Here, we present numerical model simulations of early GrIS history and show that interactions among climate, the growing ice sheet, and preexisting topography may have contributed to the excavation of the canyon via repeated catastrophic outburst floods. Our results have implications for interpreting sedimentary and geomorphic features beneath the GrIS and around its marine margins, and they document a novel mechanism for landscape erosion in Greenland.

## INTRODUCTION

Subglacial topography is a primary control on ice-sheet dynamics, and it is an important boundary condition for ice-sheet simulations (Morlighem et al., 2014). The subglacial landscape in Greenland contains complex canyon networks, which are thought to have a fluvial origin (Bamber et al., 2013; Cooper et al., 2016; Livingstone et al., 2017). The Northeast Greenland Ice Stream (NEGIS) is characterized by fast flow that is not constrained to bedrock canyons upstream but instead is thought to overlie deformable sediments (Christianson et al., 2014). In northwest Greenland, a prominent bedrock trough extends ~750 km inland from the terminus of Petermann Glacier (Fig. 1; Bamber et al., 2013), affecting subglacial water routing at the bed.

The morphology of this V-shaped canyon suggests it was formed by running water prior to extensive glaciation (Bamber et al., 2013; Cooper et al., 2016). While offshore sediment records show that the extent and duration of ice cover in the Northern Hemisphere increased ~2.7 m.y. ago, it is possible that Greenland

hosted land-based ice as early as the late Eocene (DeConto et al., 2008), and persistent ice cover over the past 7 m.y. (Bierman et al., 2016). Yet, basal material from below the Greenland ice sheet (GrIS) summit suggests episodic ice-free conditions in most of Greenland throughout the Pleistocene (Schaefer et al., 2016). Overall, the temporal and spatial history of ice cover remains controversial, including how it relates to the timing and mechanism(s) of megacanyon formation.

Here, based on ice-sheet model simulations of early GrIS history, we show that climate and bedrock topography exerted strong controls on GrIS inception. As a consequence of this coupling, GrIS inception may have been accompanied by repeated, catastrophic drainage of large proglacial meltwater lakes, presenting a new mechanism for the formation of the megacanyon.

# **METHODS**

We set up a numerical model simulation of ice-sheet evolution in Greenland, starting from a preglacial configuration with ice-free conditions in Greenland. Our simulations included interactions among climate, the ice sheet, and bedrock topography, using a regional climate model (RCM) in a one-way coupling with an ice-sheet flow model that included an Earth deformation model. Ice-sheet model output was used to calculate water-routing pathways and estimate the erosional potential of predicted paleolakes.

#### **Climate Forcing**

To generate climate forcing for the ice-sheet model, we used the GENESIS general circulation model (GCM; Alder et al., 2011), run in a slab ocean configuration using an ice-free Northern Hemisphere topography and the modern orbit. The GCM was run for 60 model years (~30 yr beyond equilibrium), saving 6 hourly output data sets to drive an RCM (Pal et al., 2007) run at 40 km resolution. We used deglaciated boundary conditions to run the RCM, i.e., isostatically equilibrated bedrock with small glaciers restricted to the eastern mountains (see the Supplemental Material<sup>1</sup>). The RCM climatology was based on a 10 year average of the deglacial temperature and precipitation fields.

To force the ice-sheet model through glacial-interglacial cycles, we generated synthetic temperature anomalies from sinusoids with a period of 41 k.y. that varied from warm interglacial-like temperatures to cool glacial-like temperatures and applied this as a spatially uniform temperature offset to the ice-free RCM climatology at each time step (Fig. 2). Our approximation of glacial-interglacial climate change took into account three fundamental characteristics of global climate evolution over the period during which

CITATION: Keisling, B.A., et al., 2020, Pliocene–Pleistocene megafloods as a mechanism for Greenlandic megacanyon formation: Geology, v. 48, p. 737–741, https://doi.org/10.1130/G47253.1

<sup>&#</sup>x27;Supplemental Material. Description of coupling between models, ice-sheet model parameters used, and calculation of erosion rates. Please visit https://doi.org/10.1130/GEOL.26213S.12132795 to access the supplemental material, and contact editing@geosociety.org with any questions. The simulations described in the text are available from the coauthors upon request.

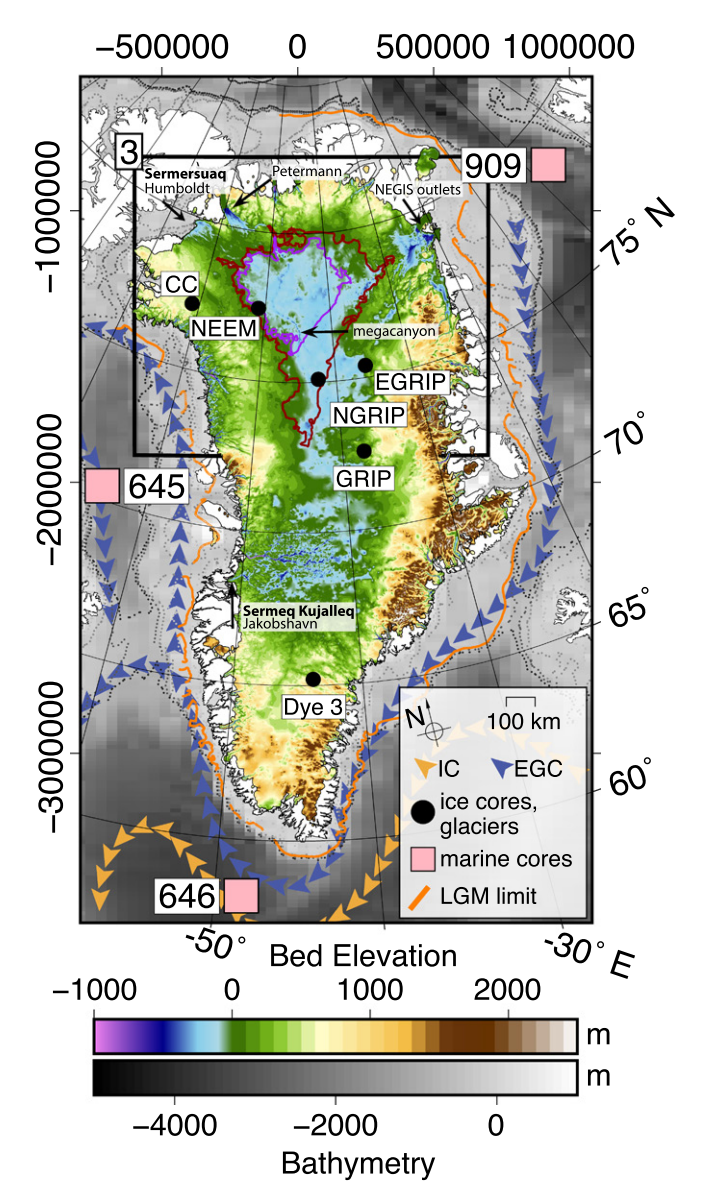


Figure 1. Map of Greenland, where gray shows ocean bathymetry, and colors show modern bed elevation beneath the Greenland ice sheet (GrIS). Red and purple outlines indicate extent of proglacial lakes in Figure 3. Ice-core and Ocean Drilling Program (ODP) sites are labeled, along with other features, including major glaciers (Bjørk et al., 2015). Orange line shows estimate of Last Glacial Maximum (LGM) ice-sheet extent (Funder et al., 2011). Black box indicates extent of maps in Figure 3. Blue and orange arrows indicate paths of (cold) East **Greenland Current (EGC)** and (warm) Irminger Current (IC), respectively (Straneo et al., 2012). Coordinate system is Polar Stereographic (EPSG 3413). CC-Camp Century; GRIP-Greenland Ice Core Project; EGRIP—East Greenland Ice Core Project: NEGIS-Northeast Greenland Ice Stream; NEEM—North Greenland Eemian Ice Drilling; NGRIP—North Greenland Ice Core Project.

the GrIS became a persistent continental-scale ice sheet (Lisiecki and Raymo, 2007): Glacial periods became increasingly colder, glacials were more variable than interglacial periods, and ran-

domly occurring "super-interglacials" caused enhanced warming. This ice-sheet forcing approach mimics the effects of orbital cyclicity on GrIS surface mass balance (SMB) over 1.2 m.y. (Fig. 2).

## Ice-Sheet Model

We used the Parallel Ice Sheet Model (PISM, pism-docs.org; Bueler and Brown, 2009), a three-dimensional thermomechanically coupled ice-sheet model. The model includes a widely used Earth deformation model with an elastic lithosphere and a relaxing asthenosphere (Greve, 2001). The model was run at 10 km resolution, with the climate forcing described above, which followed the approach in the SeaRISE assessment (adding anomaly fields using a positive degree-day [PDD] scheme for SMB; e.g., Greve et al., 2011; Nowicki et al., 2013). The PDD is a computationally efficient scheme that calculates SMB from the applied temperature field. The PDD scheme used coefficients of 3 and 8 mm °C<sup>-1</sup> d<sup>-1</sup> for melting of snow and ice, respectively, and surface temperature was adjusted to the ice-sheet geometry using a lapse rate of 5 °C km<sup>-1</sup>. We used a fixed calving margin set at the mapped Last Glacial Maximum (LGM) moraine; i.e., the ice sheet was not allowed to advance into the ocean beyond its LGM extent (Funder et al., 2011). The discharge was calculated as the calving flux over the fixed calving margin, so there was no additional ocean forcing included in this simplified model setup. The modeled discharge rates varied over time as a result of inland ice dynamics and SMB, and not from direct oceanic forcing. These choices enabled us to run multiple realizations of ice-sheet inception on time scales of millions of years.

#### Water Routing and Erosion

To reconstruct high-resolution paleotopographies, we calculated lithospheric deflection by subtracting the bedrock elevation simulated at each time step from its modern value. This field was downscaled to the resolution of available interpolated bed products (150 m; Morlighem et al., 2017) to calculate hydrologic flow paths based on local topographic gradients (Schwanghart and Scherler, 2014; TopoToolbox, at https://topotoolbox.wordpress.com/). We calculated all of the marine-terminating stream networks for

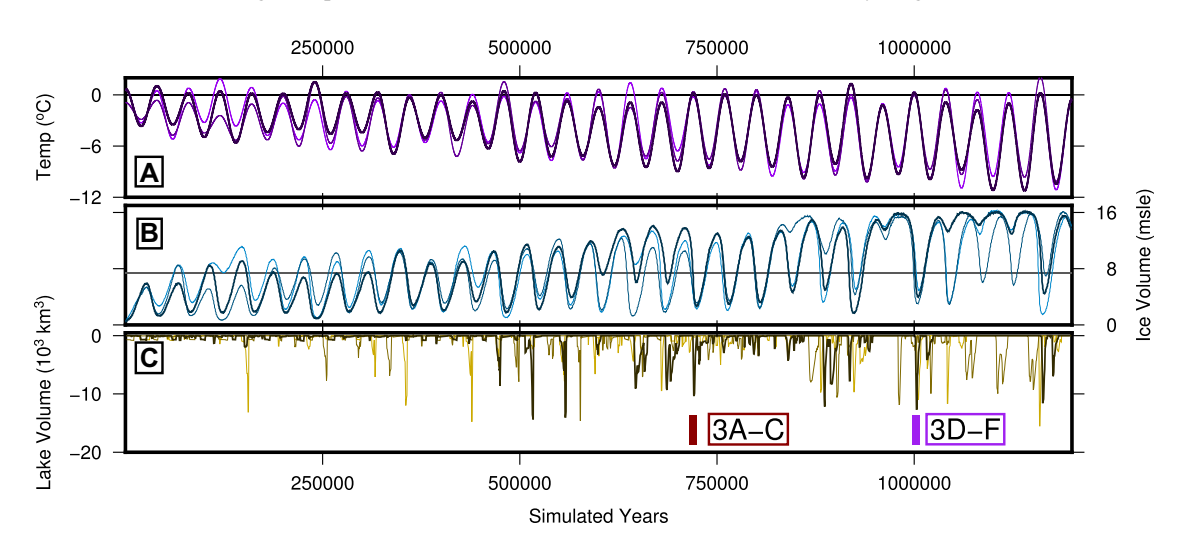


Figure 2. Temperature anomaly applied to preglacial climate state (A), Greenland ice sheet (GrIS) volume (B), and proglacial lake volume (C) for our simulations. Values above 0 °C in A mimic "superinterglacials." Simulation shown in Figure 3 is plotted with darkest, thickest line in each panel. Two other realizations are shown with thinner medium- and lighthued lines. Red and purple boxes are time slices shown in Figure 3; msle-m sea-level equivalent.

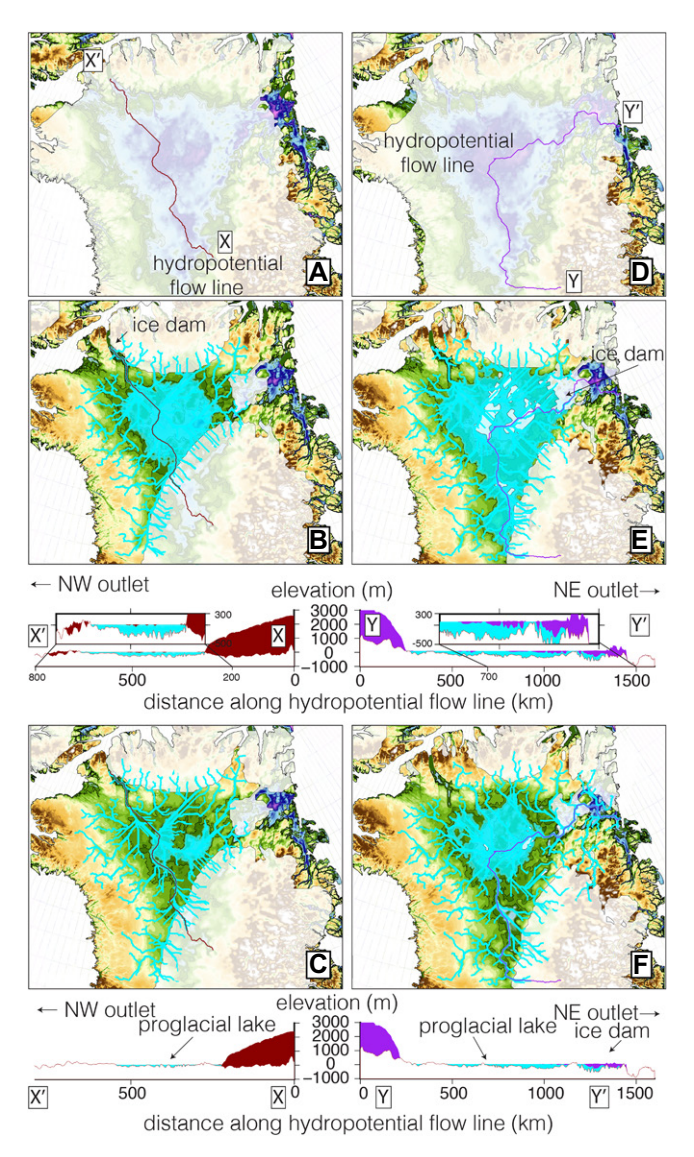


Figure 3. Development and evolution of proglacial lakes following Greenland ice sheet (GrIS) retreat. Colors (same as in Fig. 1) indicate isostatically adjusted topography, where white transparent shading shows extent of ice sheet, and turquoise lines/polygons show meltwater routing and proglacial lake extent. First row shows extent of ice sheet just prior to deglaciation. Second and third rows show proglacial lake evolution during two deglaciation phases (A-C and D-F). Subtle differences in topography dictate direction of lake outflow. Panels A-F represent 680, 687, 690, 1000, 1004, and 1008 k.y. simulated years.

deglaciated topographies to define proglacial lake catchments. Then, starting from the marine terminus of the stream network, we defined a sill as the highest landward topographic maximum above sea level, including topographic features beneath any remnant ice caps that could block outflow. This sill elevation defined the maximum depth and volume of a proglacial lake at each time step instantaneously. Uncertainties in both the Earth model and mapped bed elevations would affect the exact location of the sill; however, our goal was to highlight a potential mechanism governed by ice-sheet-climate—solid-earth feedbacks rather than to precisely identify past sill locations.

We used two approaches to estimate erosion from ice-sheet model output. First, we used modern studies of bedrock erosion caused by catastrophic floods to constrain the magnitude of landscape change we would expect from our modeled flood volumes. Second, we used a parameterization that predicts spillway erosion rate (Garcia-Castellanos and O'Connor, 2018).

We considered the range of possible values for uncertain parameters to provide a rough estimate of erosion rates for our modeled flood volumes (see the Supplemental Material).

#### RESULTS

In our simulations, the oscillating climate led to fluctuations in ice-sheet volume, but the general cooling trend contributed to the progressive establishment of the GrIS (Fig. 2). After ~600 k.y. of simulation, the GrIS volume oscillated between modern (6-8 m sea-level equivalent [s.l.e.]) during interglacial periods and larger (12–14 m s.l.e.) during glacial periods. For the largest glacial ice sheets, a warmer-than-average interglacial period was necessary to trigger a deglaciation, and the GrIS was able continue to grow through multiple glacial-interglacial cycles (Fig. 2). During these skipped interglacial periods, the bedrock continued its isostatic adjustment to the increased ice load, leading to the development of an overdeepened basin in central Greenland with subglacial outlets in both

the northwest (via Petermann) and the northeast (via NEGIS; Fig. 1). This basin had the largest volume following a skipped interglacial, but it was observed throughout our simulations during deglaciations (Fig. 3).

When a warm interglacial occurs after a period of prolonged stability, the GrIS rapidly disintegrates due to the positive SMB-elevation feedback (Weertman, 1961), and the ice retreats into regions with submarine bed elevations. Large parts of western Greenland, i.e., within the modern-day ablation zone, begin to melt due to surface imbalance. As mass loss continues, the GrIS retreats along troughs in the northwest and northeast, creating a saddle that rapidly ablates, revealing a large subaerial basin with direct access to the ocean blocked by small remnant ice caps (i.e., ice dams; Fig. 3). Variations in the thickness of ice in northeast and northwest Greenland prior to deglaciation determine whether the first ice-free route is observed through the Petermann canyon or the outlets of NEGIS (Fig. 3).

Based on the outcropping lithified sedimentary rocks mapped in ice-free regions of North Greenland (Dawes, 2004), we assume that the erodibility of the bedrock in North Greenland is low (Garcia-Castellanos and O'Connor, 2018). Taking the isostatically compensated channel slope  $(0.3 \times 10^{-3}$ ; Bamber et al., 2013) and estimating 100 m water elevation above sill height prior to an outburst flood (Figs. 3B and 3E), we predict spillway erosion rates ranging from 0.5 to 5 m yr<sup>-1</sup> in response to outburst flooding (see the Supplemental Material).

# DISCUSSION

Though PISM is a complex model capable of realistically simulating the dynamics of modern ice sheets (i.e., Aschwanden et al., 2016), we used it here not to depict reality but as a tool to explore feedbacks in the climate-ice sheet-bedrock system following glaciation. Our simulations point to an erosive mechanism that has been recognized for the formation of other large proglacial canyon networks in North America (Larsen and Lamb, 2016) but not yet considered for the landscape beneath the GrIS. Thus, although we cannot date canyon formation, our results provide a framework for understanding Greenland's landscape evolution via linked geomorphologic, climatic, and glaciologic processes, and they provide a new hypothesis that can be tested by additional modeling and targeted field studies.

# Megacanyon Formation via Repeated Proglacial Lake Outburst Floods

Following the LGM, meltwater lakes left by retreating Northern Hemisphere ice sheets caused catastrophic floods that altered surrounding landscapes (Larsen and Lamb, 2016; Teller et al., 2002; Clarke et al., 2004). During the Holocene, erosive glacial outburst floods have estimated minimum discharge rates of  $10^{-3}$ – $10^{-2}$  Sv ( $10^6$  m³/s), or ~ $10\times$  lower than those estimated for LGM floods (Grinsted et al., 2017; Walder and Costa, 1996). Our simulations predict that during periods of rapid GrIS retreat following glacial maxima, subaerial meltwater lakes formed in northern Greenland with a similar volume to erosive, and climatically disruptive, proglacial lakes in North America following the LGM (Teller et al., 2002).

According to our calculations, erosion rates in response to these outburst floods would be 0.5–5 m yr<sup>-1</sup> (see the Supplemental Material). The maximum depth of the Petermann canyon is ~800 m, requiring 160-1600 yr of flood-style erosion, which could be accomplished over more than one interglacial and up to tens of interglacials. Observations of modern catastrophic floods provide another constraint on the total erosion by this mechanism. The estimated discharge for the floods we propose (0.6 Sv) is two orders of magnitude higher than catastrophic floods in the historical record that caused tens of meters of vertical erosion over kilometers (Lamb and Fonstad, 2010; Wilson et al., 2019). If we assume that the higher discharge of the floods we reconstructed had a similar erosive potential over a larger spatial scale, with 1-20 m of vertical erosion per flood event, our mechanism requires 40-800 jökulhlaup-like floods, consistent with the physically motivated estimate of canyon incision occurring over multiple interglacials (see the Supplemental Material).

# Comparison with Marine Sedimentary Records

Marine sediments are a potential source of information about past outburst floods. Seismic studies have mapped Pliocene-Pleistocene sediment packages north of Greenland that may reflect periods of enhanced terrestrial erosion. In northern Baffin Bay, high-resolution seismic surveys revealed thick Pliocene- and Pleistocene-age deposits, dated by regional correlation of seismic reflectors to Ocean Drilling Program (ODP) Site 645 (Knutz et al., 2015). Off northeast Greenland, in the Boreas (77°N-79°N) and Molloy (79°N-80°N) Basins, sedimentation rates tripled from 3.4 to 10.3 cm k.y.<sup>-1</sup> during the Pliocene, falling to 7.3 cm k.y.<sup>-1</sup> during the late Pliocene and Pleistocene (Berger and Jokat, 2009). One explanation for this change in sedimentation rate is provided by early, successive, and erosive glaciations in Greenland, consistent with the periodic outburst mechanism proposed here.

Ice-rafted debris (IRD) can reflect iceberg discharge, and IRD layers are often associated with high meltwater discharge volumes that promote iceberg transport (Teller et al., 2002). Thus, although equivocal, IRD may also carry the signature of past outburst floods originating

from Greenland. At ODP Site 645, IRD is present throughout the Pliocene–Pleistocene. In the early Pliocene, 10% of the sediments consist of up to 1-m-thick beds attributed to rapid emplacement of poorly sorted sandy sediment (Hiscott et al., 1989b), interpreted as debris-flow or iceberg discharge events. Because the provenance of some IRD in the Pleistocene section of the core points directly to a source in northern Greenland, Thule Basin (Hiscott et al., 1989a), we suggest these beds may also be linked to outburst flood events originating in North Greenland (Fig. 3).

#### **CONCLUSIONS**

We used a numerical model to simulate the initiation of the GrIS and show the potential for interactions among climate, ice sheets, and bedrock topography to cause erosive outburst floods. Based on inferred proglacial lake volumes and realistic discharge rates, we hypothesize that Petermann canyon may have been formed by tens to hundreds of Pleistocene flood events similar to those documented for other ice sheets during previous deglaciations. These floods present a plausible scenario for the formation of the largest mapped subglacial feature in Greenland. Future work on marine sediment cores from around Greenland can directly test this hypothesis. If the occurrence of outburst floods can be confirmed with physical evidence, it will alter our understanding of linkages between landscape denudation and GrIS evolution.

# ACKNOWLEDGMENTS

Figures were made using the Generic Mapping Toolbox. Development of the Parallel Ice Sheet Model (PISM, pism-docs.org) was supported by NASA grants NNX13AM16G and NNX13AK27G. Keisling was funded by the U.S. National Science Foundation (NSF) through grant GRF-1451512, a GROW Fellowship (NSF/Danish National Research Foundation [DNRF]), and NSF grant ARC-1417886. The Centre for Ice and Climate is funded by the Danish National Research Foundation (DNRF). We thank three anonymous reviewers for their feedback, and C. Clark for serving as editor.

# REFERENCES CITED

- Alder, J.R., Hostetler, S.W., Pollard, D., and Schmittner, A., 2011, Evaluation of a presentday climate simulation with a new coupled atmosphere-ocean model GENMOM: Geoscientific Model Development, v. 4, p. 69–83, https://doi .org/10.5194/gmd-4-69-2011.
- Aschwanden, A., Fahnestock, M.A., and Truffer, M., 2016, Complex Greenland outlet glacier flow captured: Nature Communications, v. 7, 10524, https://doi.org/10.1038/ncomms10524.
- Bamber, J.L., Siegert, M.J., Griggs, J.A., Marshall, S.J., and Spada, G., 2013, Paleofluvial mega-canyon beneath the central Greenland ice sheet: Science, v. 341, p. 997–999, https://doi.org/10.1126/ science.1239794.
- Berger, D., and Jokat, W., 2009, Sediment deposition in the northern basins of the North Atlantic and characteristic variations in shelf sedimentation along the East Greenland margin: Marine and Petroleum Geology, v. 26, p. 1321–1337, https:// doi.org/10.1016/j.marpetgeo.2009.04.005.

- Bierman, P.R., Shakun, J.D., Corbett, L.B., Zimmerman, S.R., and Rood, D.H., 2016, A persistent and dynamic East Greenland ice sheet over the past 7.5 million years: Nature, v. 540, p. 256–260, https://doi.org/10.1038/nature20147.
- Bjørk, A.A., Kruse, L.M., and Michaelsen, P.B., 2015, Brief communication: Getting Greenland's glaciers right—A new data set of all official Greenlandic glacier names: The Cryosphere, v. 9, p. 2215–2218, https://doi.org/10.5194/tc-9-2215-2015.
- Bueler, E., and Brown, J., 2009, Shallow shelf approximation as a "sliding law" in a thermomechanically coupled ice sheet model: Journal of Geophysical Research: Earth Surface, v. 114, F03008, https://doi.org/10.1029/2008JF001179.
- Christianson, K., Peters, L.E., Alley, R.B., Anandakrishnan, S., Jacobel, R.W., Riverman, K.L., Muto, A., and Keisling, B.A., 2014, Dilatant till facilitates ice-stream flow in northeast Greenland: Earth and Planetary Science Letters, v. 401, p. 57–69, https://doi.org/10.1016/ j.epsl.2014.05.060.
- Clarke, G.K.C., Leverington, D.W., Teller, J.T., and Dyke, A.S., 2004, Paleohydraulics of the last outburst flood from glacial Lake Agassiz and the 8200 BP cold event: Quaternary Science Reviews, v. 23, p. 389–407, https://doi.org/10.1016/j.quascirev.2003.06.004.
- Cooper, M.A., Michaelides, K., Siegert, M.J., and Bamber, J.L., 2016, Paleofluvial landscape inheritance for Jakobshavn Isbræ catchment, Greenland: Geophysical Research Letters, v. 43, p. 6350–6357, https://doi.org/10.1002/2016GL069458.
- Dawes, P.R., 2004, Explanatory Notes to the geological Map of Greenland, 1:500 000, Humboldt Gletscher, Sheet 6: Geological Survey of Denmark and Greenland (GEUS) Greenland Map Series 1, 48 p.
- DeConto, R.M., Pollard, D., Wilson, P.A., Pälike, H., Lear, C.H., and Pagani, M., 2008, Thresholds for Cenozoic bipolar glaciation: Nature, v. 455, p. 652–656, https://doi.org/10.1038/nature07337.
- Funder, S., Kjeldsen, K.K., Kjær, K.H., and Ó Cofaigh, C., 2011, The Greenland ice sheet during the past 300,000 years: A review, in Ehlers, J., et al., eds., Quaternary Glaciations—Extent and Chronology: A Closer Look: Amsterdam, Elsevier, Developments in Quaternary Sciences 15, p. 699–713, https://doi.org/10.1016/B978-0-444-53447-7.00050-7.
- Garcia-Castellanos, D., and O'Connor, J.E., 2018, Outburst floods provide erodability estimates consistent with long-term landscape evolution: Scientific Reports, v. 8, 10573, https://doi .org/10.1038/s41598-018-28981-y.
- Greve, R., 2001, Glacial isostasy: Models for the response of the Earth to varying ice loads, *in* Straughan B., et al., eds., Continuum Mechanics and Applications in Geophysics and the Environment: Berlin, Springer, p. 307–325, https://doi.org/10.1007/978-3-662-04439-1\_16.
- Greve, R., Saito, F., and Abe-Ouchi, A., 2011, Initial results of the SeaRISE numerical experiments with the models SICOPOLIS and IcIES for the Greenland ice sheet: Annals of Glaciology, v. 52, p. 23–30, https://doi.org/10.3189/172756411797252068.
- Grinsted, A., Hvidberg, C.S., Campos, N., and Dahl-Jensen, D., 2017, Periodic outburst floods from an ice-dammed lake in East Greenland: Scientific Reports, v. 7, 9966, https://doi.org/10.1038/ s41598-017-07960-9.
- Hiscott, R.N., Aksu, A.E., and Nielsen, O.B., 1989a, Provenance and dispersal patterns, Pliocene— Pleistocene section at Site 645, Baffin Bay, *in* Srivastava, S.P., et al., Proceedings of the Ocean

- Drilling Program: Scientific Results, Volume 105: College Station, Texas, Ocean Drilling Program, https://doi.org/10.2973/odp.proc.sr.105.117.1989.
- Hiscott, R.N., Cremer, M., and Aksu, A.E., 1989b, Evidence from sedimentary structures for processes of sediment transport and deposition during post-Miocene time at Sites 645, 646, and 647, Baffin Bay and the Labrador Sea, *in* Srivastava, S.P., et al., Proceedings of the Ocean Drilling Program: Scientific Results, Volume 105: College Station, Texas, Ocean Drilling Program, p. 53–63, https://doi.org/10.2973/odp.proc.sr.105.119.1989.
- Knutz, P.C., Hopper, J.R., Gregersen, U., Nielsen, T., and Japsen, P., 2015, A contourite drift system on the Baffin Bay–West Greenland margin linking Pliocene Arctic warming to poleward ocean circulation: Geology, v. 43, p. 907–910, https:// doi.org/10.1130/G36927.1.
- Lamb, M.P., and Fonstad, M.A., 2010, Rapid formation of a modern bedrock canyon by a single flood event: Nature Geoscience, v. 3, p. 477–481, https://doi.org/10.1038/ngeo894.
- Larsen, I.J., and Lamb, M.P., 2016, Progressive incision of the Channeled Scablands by outburst floods: Nature, v. 538, p. 229–232, https://doi.org/10.1038/nature19817.
- Lisiecki, L.E., and Raymo, M.E., 2007, Plio–Pleistocene climate evolution: Trends and transitions in glacial cycle dynamics: Quaternary Science Reviews, v. 26, p. 56–69, https://doi.org/10.1016/j.quascirev.2006.09.005.
- Livingstone, S.J., Chu, W., Ely, J.C., and Kingslake, J., 2017, Paleofluvial and subglacial channel

- networks beneath Humboldt Glacier, Greenland: Geology, v. 45, p. 551–554, https://doi.org/10.1130/G38860.1.
- Morlighem, M., Rignot, E., Mouginot, J., Seroussi, H., and Larour, E., 2014, Deeply incised submarine glacial valleys beneath the Greenland ice sheet: Nature Geoscience, v. 7, p. 418–422, https://doi.org/10.1038/ngeo2167.
- Morlighem, M., et al., 2017, BedMachine v3: Complete bed topography and ocean bathymetry mapping of Greenland from multibeam echo sounding combined with mass conservation: Geophysical Research Letters, v. 44, p. 11051–11061, https://doi.org/10.1002/2017GL074954.
- Nowicki, S., et al., 2013, Insights into spatial sensitivities of ice mass response to environmental change from the SeaRISE ice sheet modeling project II: Greenland: Journal of Geophysical Research: Earth Surface, v. 118, p. 1025–1044, https://doi.org/10.1002/jgrf.20076.
- Pal, J.S., et al., 2007, Regional climate modeling for the developing world: The ICTP RegCM3 and RegCNET: Bulletin of the American Meteorological Society, v. 88, p. 1395–1410, https://doi .org/10.1175/BAMS-88-9-1395.
- Schaefer, J.M., Finkel, R.C., Balco, G., Alley, R.B., Caffee, M.W., Briner, J.P., Young, N.E., Gow, A.J., and Schwartz, R., 2016, Greenland was nearly ice-free for extended periods during the Pleistocene: Nature, v. 540, p. 252–255, https:// doi.org/10.1038/nature20146.
- Schwanghart, W., and Scherler, D., 2014, Short Communication: TopoToolbox 2—MATLABbased software for topographic analysis and

- modeling in Earth surface sciences: Earth Surface Dynamics, v. 2, p. 1–7, https://doi.org/10.5194/esurf-2-1-2014.
- Straneo, F., Sutherland, D.A., Holland, D., Gladish, C., Hamilton, G.S., Johnson, H.L., Rignot, E., Xu, Y., and Koppes, M., 2012, Characteristics of ocean waters reaching Greenland's glaciers: Annals of Glaciology, v. 53, p. 202–210, https:// doi.org/10.3189/2012AoG60A059.
- Teller, J.T., Leverington, D.W., and Mann, J.D., 2002, Freshwater outbursts to the oceans from glacial Lake Agassiz and their role in climate change during the last deglaciation: Quaternary Science Reviews, v. 21, p. 879–887, https://doi.org/10.1016/S0277-3791(01)00145-7.
- Walder, J.S., and Costa, J.E., 1996, Outburst floods from glacier-dammed lakes: The effect of mode of lake drainage on flood magnitude: Earth Surface Processes and Landforms, v. 21, p. 701–723, https://doi.org/10.1002/(SICI)1096-9837(199608)21:8<701::AID-ESP615>3.0.CO;2-2.
- Weertman, J., 1961, Stability of ice-age ice sheets: Journal of Geophysical Research, v. 66, p. 3783–3792, https://doi.org/10.1029/JZ066i011p03783.
- Wilson, R., Harrison, S., Reynolds, J., Hubbard, A., Glasser, N.F., Wündrich, O., Iribarren Anacona, P., Mao, L., and Shannon, S., 2019, The 2015 Chileno Valley glacial lake outburst flood, Patagonia: Geomorphology, v. 332, p. 51–65, https://doi.org/10.1016/j.geomorph.2019.01.015.

Printed in USA